ALT 12
Advanced Laser Technologies
2 – 6 September 2012, Thun, Switzerland

ALT 12
c/o Bern University of Applied Sciences
Engineering and Information Technology
Pestalozzistrasse 20, CH-3400 Burgdorf
info@alt12.org, www.alt12.org
0041 (0) 34 426 42 06

THE RESONANCE FLUORESCENCE SPECTRA OF N TWO-LEVEL QUANTUM SYSTEMS LOCATED AROUND THE SPHERICAL NANOANTENNA

Authors:

Yu.V. Vladimirova, V.V. Klimov, V.M. Pastukhov, V.N. Zadkov

DOI: 10.12684/alt.1.85

Corresponding author: Yu.V. Vladimirova

e-mail: yu.vladimirova@physics.msu.ru

The resonance fluorescence spectra of N two-level quantum systems located around the spherical nanoantenna

Yu.V. Vladimirova[1], V.V. Klimov[2], V.M. Pastukhov[1], V.N. Zadkov[1]
[1]International Laser Center and Faculty of Physics,
M.V. Lomonosov Moscow State University, Moscow 119991, Russia
[2]P.N. Lebedev Physical Institute, Russian Academy of Sciences,
Leninsky ave. 53, 119991 Moscow, Russia

Abstract

Modification of the resonance fluorescence spectrum of a two-level atom driving by a laser monochromatic field in the close proximity of a plasmonic nanostructure (metal sphere) is studied in detail. It is shown that one can control this spectrum varying four key parameters: distance between the atom and the nanosphere, atom's location around the nanosphere, the radius of the nanosphere, and polarization of the incident radiation. These parameters affect the local field enchancement, transition frequency shift and the modification of the radiative decay rate of the atom interacting with the nanosphere, which lead to modification of the resonance fluorescence spectrum of the atom (frequency shift of the satellite lines in the Mollow-type triplet, widths of the lines, the spectrum intensity) by contrast with that one in free space. The permittivity of the metal the nanosphere is made of is also an additional parameter, which defines the nonradiative decay. The latter in combination with other parameters allows to continuously control the transition from resonance fluorescence enhancement to its quenching. The calculation results are generalized to the case of N two-level atoms, distributed around the nanoparticle in the close proximity of its surface. The calculations were performed for different positions of the detector relative to the system nanoparticle-atom(s).

Introduction

Since the early indication by Sommerfeld [1] and then the pioneering work of Purcell [2] it is well known that the radiative properties of an emitter (specifically, atom, molecule or quantum dot) are strongly modified in the confined geometries [3, 4]). Of special interest is interaction of atoms and molecules with plasmonics nanostructures. It has been shown that the plasmonic nanostructures work not only as optical antennas converting the incoming radiation to localized energy and vice versa generating spots of significant enchancement of the local field, but also the lifetime of an excited quantum emitter located near the nanostructure is affected by the radiative decay rate due to photon emission and by the nonradiative decay rate due to energy dissipation in the environment and both these rates for atoms and molecules closed to metal surfaces can be enhanced [5, 6, 7, 8, 9, 10, 11].

Most fluorescence studies of a single atom, molecule or quantum dot have been done using spontaneous fluorescence. Key advantage of the resonant fluorescence by contrast with the spontaneous one is that the resonance fluorescence exhibits much more information about the system under study, including quantum features of interaction of the incident radiation with the system [15].

The arrangement of the atom–nanosphere–incident field system is given in Fig. 1. A two-level atom with ground and excited states and with the dipole moment $\mathbf{d}$ is placed in close proximity to the metal nanosphere of radius a. The atom's location around the nanosphere is defined by its radial coordinate $|\mathbf{r}|$ and the polar angle θ (in spherical coordinate system), ε and ε_2 are the permittivities of the metal the nanosphere is made of and the space our system of atom–nanosphere is placed in, respectively [16]. To be more specific, we will assume that the nanosphere is made of silver, i.e., its

permittivity is equal to $\varepsilon = -15.37 + i0.231$ and the wavelength of the incident laser field $\lambda = 632.8$ nm. We will also assume for simplicity that $\varepsilon_2 = 1$. The incoming z-polarized electromagnetic radiation $\mathbf{E}_{\rm inc}$ at the frequency ω_L, which is closed to the frequency ω_0 of the the atomic dipole transition from ground to the excited state, has the wavevector $\mathbf{k}$ directed along y-axis. It is important to note also that the direction of the atomic dipole moment coincides with the direction of the local field created by the (atom–nanosphere–excited radiation) system in the point of space the atom is located.

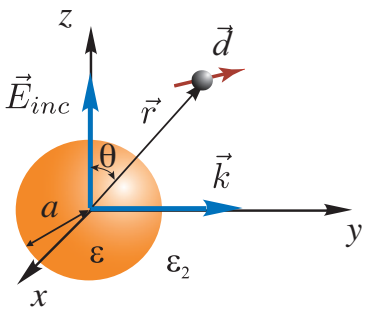

Figure 1: Arrangement of the problem

The atom's excitation and radiative/nonradiative decay rates near the plasmonic nanostructure

Electric field intensity in the close proximity to the nanobody, which size is significantly less than the wavelength $\lambda = 632.8$ nm of the incoming field, can be calculated in the quasistatic approximation, which implies that no retardation effects are taken into account.

For the nanosphere of radius $a = 20$ nm in the homogeneous incident electric field only dipole resonances with $n = 1$ are excited and the field inside the nanosphere is equal to

$$\mathbf{E} = E_r\hat{\mathbf{n}}_r + E_\theta\hat{\mathbf{n}}_\theta = E_0\frac{3}{\varepsilon(\omega)+2}(\cos\theta\hat{\mathbf{n}}_r - \sin\theta\hat{\mathbf{n}}_\theta), \quad (1)$$

whereas outside the nanosphere it becomes

$$\mathbf{E} = E_r\hat{\mathbf{n}}_r + E_\theta\hat{\mathbf{n}}_\theta = E_0(\cos\theta\hat{\mathbf{n}}_r - \sin\theta\hat{\mathbf{n}}_\theta) + \\ + E_0\frac{a^3}{r^3}\frac{\varepsilon(\omega)-1}{\varepsilon(\omega)+2}(2\cos\theta\hat{\mathbf{n}}_r + \sin\theta\hat{\mathbf{n}}_\theta), \quad (2)$$

where E_0 is the amplitude of the incident filed and $\hat{\mathbf{n}}_r$, $\hat{\mathbf{n}}_\theta$ are the unit vectors in spherical coordinate system, $\varepsilon(\omega)$ is the permittivity of the nanobody at the frequency ω, $\mathbf{E}_{\rm inc}$ is the incident field, field $\hat{\mathbf{e}}_n$ describes the eigen oscillations of the body filling the volume V with the permittivity ε_n and n is the vector index, which defines the specific plasmonic mode. It is also worth to note here that in the case of sphere $E_\phi = 0$.

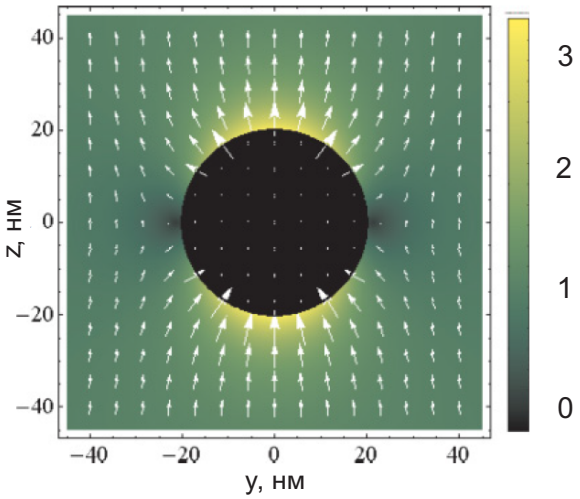

Figure 2: (Color online) Distribution of the field $\mathbf{E}$ vectors mapped on the total density of the field in the vicinity of silver nanosphere in yz plane, calculated by Eq. (2). Sphere radius $a = 20$ nm, $\lambda = 632.8$ nm, the incident field is polarized along z-axis

In the external electromagnetic field, the dipole moment of the atom is directed along the direction of the field in the point of space the atom is located. From Fig. 2, which shows the distribution of the local field vectors in the vicinity of the nanosphere, one can clearly see that the direction of the local field and its intensity essentially depend on $\mathbf{r}$, so that the Rabi frequency Ω also depends on $\mathbf{r}$ and can be written as

$$\Omega(\mathbf{r}) = \frac{d}{\hbar}\sqrt{|E_r|^2 + |E_\theta|^2 + |E_\varphi|^2}, \quad (3)$$

which with the help of Eq. (2) takes the form

$$\Omega(\mathbf{r}) = \frac{d}{\hbar}\sqrt{|E_r|^2 + |E_\theta|^2} = \\ = \frac{d}{\hbar}\Big(\Big|E_0\cos\theta\Big(\frac{2a^3}{r^3}\frac{\varepsilon(\omega)-1}{\varepsilon(\omega)+2}+1\Big)\Big|^2 + \\ + \Big|E_0\sin\theta\Big(\frac{a^3}{r^3}\frac{\varepsilon(\omega)-1}{\varepsilon(\omega)+2}-1\Big)\Big|^2\Big)^{1/2}, \quad (4)$$

where the atomic dipole transition moment is equal (in gaussian system of units) to

$$d = \left(\frac{3\gamma_0\hbar c^3}{4\omega_0^3}\right)^{\frac{1}{2}}, \quad (5)$$

ω_0 is the frequency of the atomic dipole transition and γ_0 is the radiative decay rate of the atom in free space [15].

The total normalized linewidth of the atom located at the point with radius-vector $\mathbf{r}$ and with the atomic dipole moment directed along the direction of the local field in this point can be defined as (see [3], Section 6.3)

$$\gamma/\gamma_0 = \{\cos^2\xi(\gamma/\gamma_0)_{\rm rad} + \sin^2\xi(\gamma/\gamma_0)_{\rm tan}\}, \quad (6)$$

where $\gamma_{\rm rad}$ is the total decay rate of the atom near the nanosphere for the radial orientation of the dipole moment towards the nanosphere and $\gamma_{\rm tan}$ — for the tangential orientation, γ_0 is the natural linewidth of the atom in free space and ξ is the angle between the directions of the dipole moment and $\mathbf{r}$. Taking into account that

$$\cos^2\xi = \frac{|E_r|^2}{\sqrt{|E_r|^2+|E_\theta|^2+|E_\varphi|^2}},$$

$$\sin^2\xi = \frac{|E_\theta|^2+|E_\varphi|^2}{\sqrt{|E_r|^2+|E_\theta|^2+|E_\varphi|^2}},$$

where $(\gamma/\gamma_0)_{\rm rad}$ is the total decay rate for the radial orientation of the atomic dipole moment that can be expressed as

$$\Big(\frac{\gamma}{\gamma_0}\Big)_{\rm rad} \xrightarrow{|\mathbf{k}|a\to 0} \frac{3}{2(|\mathbf{k}||\mathbf{r}|)^3}{\rm Im}\sum_{n=1}^{\infty}(n+1)^2\cdot \\ \cdot\Big(\frac{a}{|\mathbf{r}|}\Big)^{2n+1}\frac{\alpha_n}{a^{2n+1}} + \Big|1+\frac{2\alpha_1}{|\mathbf{r}|^3}\Big|^2 + O\Big(\frac{1}{|\mathbf{k}|a}\Big) \quad (7)$$

and $(\gamma/\gamma_0)_{\rm tan}$ is the total decay rate for the tangential orientation of the atomic dipole moment, which is equal to

$$\Big(\frac{\gamma}{\gamma_0}\Big)_{\rm tan} \xrightarrow{|\mathbf{k}|a\to 0} \frac{3}{4(|\mathbf{k}||\mathbf{r}|)^3}{\rm Im}\sum_{n=1}^{\infty}n(n+1)\cdot \\ \cdot\Big(\frac{a}{|\mathbf{r}|}\Big)^{2n+1}\frac{\alpha_n}{a^{2n+1}} + \Big|1-\frac{\alpha_1}{|\mathbf{r}|^3}\Big|^2 + O\Big(\frac{1}{|\mathbf{k}|a}\Big), \quad (8)$$

where

$$\alpha_n = a^{2n+1}\frac{\varepsilon(\omega)-\varepsilon_2}{\varepsilon(\omega)+\varepsilon_2(n+1)/n} \quad (9)$$

are the multipole polarizabilities of n-th order that generalize the dipole polarizability at $n=1$.

First term in Eqs. (7) and (8) describes the nonradiation atomic decay rate, i.e., that part of the atom's energy, which is converted to the heat. The radiative decay rate of the atom is defined actually by the second term in Eqs. (7) and (8). Figure 3 shows (in logarithmic scale) how the radiative, nonradiate, and total decay rates correspond to each other for the silver nanosphere we use in our calculations.

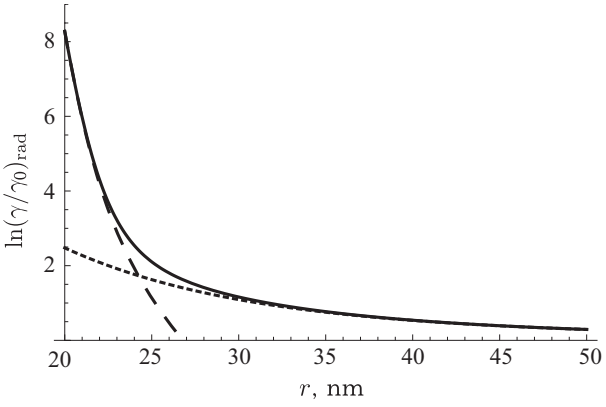

Figure 3: Radial components of the radiative (dotted line), nonradiative (dashed line) and total (solid line) decay rates for the spherical silver particle of radius $a = 20$ nm, $|\mathrm{k}|a = 0.2$, $\varepsilon = -15.37 + i0.231$ at $\lambda = 632.8$ nm

The resonance fluorescence spectrum depends on the Rabi frequency, i.e., the local field field amplitude and the direction of this field, and the total decay rate, which are all affected in the presence of the nanoparticle. The atomic resonance near the

plasmonic nanoparticle is also shifted at the frequency about the linewidth, so that for observing the resonance fluorescence one needs to adjust the incident laser frequency at the value of this frequency shift [14]. It is very important to remember about this shift when we consider the case of N emitters around the nanosphere.

For the frequency shift we have [14]:

$$\Delta\omega = -\gamma_0 \frac{3}{8} \frac{\epsilon(\omega)-1}{z^4} \sum_{n=1}^{\infty} \frac{n(n+1)}{(\epsilon(\omega)+1)n+1} \times \times \left(\frac{z_2}{z}\right)^{2n} \left[2(n+2)z_2 \cos^2\xi + nz\sin^2\xi\right], \quad (10)$$

where $z = rk$, $z_2 = ak$.

Calculation of the resonance fluorescence spectrum for a single atom

The spectrum of resonance fluorescence of a two-level atom in free space exhibits three well-separated spectral lines at sufficiently high intensity of the driving monochromatic field and coherent and homogeneously broadened incoherent lines for a weak excitation. This fluorescence triplet, which is sometime referred to as Mollow triplet, was predicted by Apanasevich [17] and then by Mollow [18], and has been observed and studied in detail experimentally (see for details [19]).

The theory of resonance fluorescence is well-developed and general approach presented in Ref. [15] can be readily applied to the case of an atom in any environment. From that theory it follows that the spectral density of the fluorescence emitted by a driven atom (resonance fluorescence) is defined by the normally ordered correlation function $\langle E^{(-)}(\mathbf{r},t)E^{(+)}(\mathbf{r},t+\tau)\rangle$ of the fluorescent light at some suitably chosen point $\mathbf{r}$ in the far-field, where $E^{(+)}(\mathbf{r},t)$, $E^{(-)}(\mathbf{r},t)$ are the positive and negative frequency parts of the electric field operator [15]:

$$S(\mathbf{r},\omega_L) = \Re \int_0^{\infty} d\tau \langle E^{(-)}(\mathbf{r},t)E^{(+)}(\mathbf{r},t+\tau)\rangle e^{i\omega_L\tau}. \quad (11)$$

For the two-level atom, the correlation function simplifies to [15]

$$\langle E^{(-)}(\mathbf{r},t)E^{(+)}(\mathbf{r},t+\tau)\rangle = = I_0(\mathbf{r})\sin^2\psi\, e^{-i\omega\tau}\Big(\frac{\Omega^2(\mathbf{r})}{\gamma^2(\mathbf{r})+2\Omega^2(\mathbf{r})}\Big)\times \times \Big[\frac{\gamma^2(\mathbf{r})}{\gamma^2(\mathbf{r})+2\Omega^2(\mathbf{r})} + \frac{e^{-\gamma\tau/2}}{2} + \frac{e^{-3\gamma\tau/4}}{4}\{e^{-i\mu(\mathbf{r})\tau}\times \times (P(\mathbf{r})+iQ(\mathbf{r})) + e^{i\mu(\mathbf{r})\tau}(P(\mathbf{r})-iQ(\mathbf{r}))\}\Big], \quad (12)$$

where $I_0(\mathbf{r}) = [(\omega^2|\mathbf{d}|)/(c^2|\mathbf{r}|)]^2$, ψ is the angle between z-axis and the direction of the dipole, which is located in the plane yz and we assume that the observer is located at z-axis, and $P = P(\mathbf{r})$, $Q = Q(\mathbf{r})$ and $\mu = \mu(\mathbf{r})$ are defined as

$$P(\mathbf{r}) = \frac{2\Omega^2(\mathbf{r})-\gamma^2(\mathbf{r})}{2\Omega^2(\mathbf{r})+\gamma^2(\mathbf{r})},$$
$$Q(\mathbf{r}) = \frac{\gamma(\mathbf{r})}{4\mu(\mathbf{r})}\frac{10\Omega^2(\mathbf{r})-\gamma^2(\mathbf{r})}{2\Omega^2(\mathbf{r})+\gamma^2(\mathbf{r})},$$
$$\mu(\mathbf{r}) = \Big(\Omega^2(\mathbf{r}) - \frac{\gamma^2(\mathbf{r})}{16}\Big)^{1/2}. \quad (13)$$

By taking the Fourier transform on $\langle E^{(-)}(\mathbf{r},t)E^{(+)}(\mathbf{r},t+\tau)\rangle$, we obtain the spectral density $S(\mathbf{r},\omega_L)$ of the electromagnetic field at $\mathbf{r}$:

$$S(\mathbf{r},\omega_L) = I_0(\mathbf{r})\Big(\frac{\Omega^2(\mathbf{r})}{\gamma^2(\mathbf{r})+2\Omega^2(\mathbf{r})}\Big)\times \times \Big[\frac{\gamma^2(\mathbf{r})}{\gamma^2(\mathbf{r})+2\Omega^2(\mathbf{r})}\delta(\omega-\omega_L) + \frac{\gamma(\mathbf{r})}{(\omega-\omega_L)^2} + + \frac{\alpha_+(\mathbf{r})}{(\omega+\mu(\mathbf{r})-\omega_L)^2} + \frac{\alpha_-(\mathbf{r})}{(\omega-\mu(\mathbf{r})-\omega_L)^2}\Big], \quad (14)$$

where

$$\alpha_\pm = \frac{3\gamma(\mathbf{r})}{4}P(\mathbf{r}) \pm (\omega \pm \mu(\mathbf{r}) - \omega_L)Q(\mathbf{r}). \quad (15)$$

The resonance fluorescence spectrum of a two-level atom near the nanosphere are shown in Figs. 4, 5.

The position of the atom located in yz-plane in the vicinity of the nanosphere is characterized by two parameters—radial coordinate $|\mathbf{r}|$ and angle θ ($\varphi = 0$).

Fig. 4 shows how the resonance fluorescence spectrum of the atom spaced from the surface of the nanosphere at 10 nm changes versus angle θ

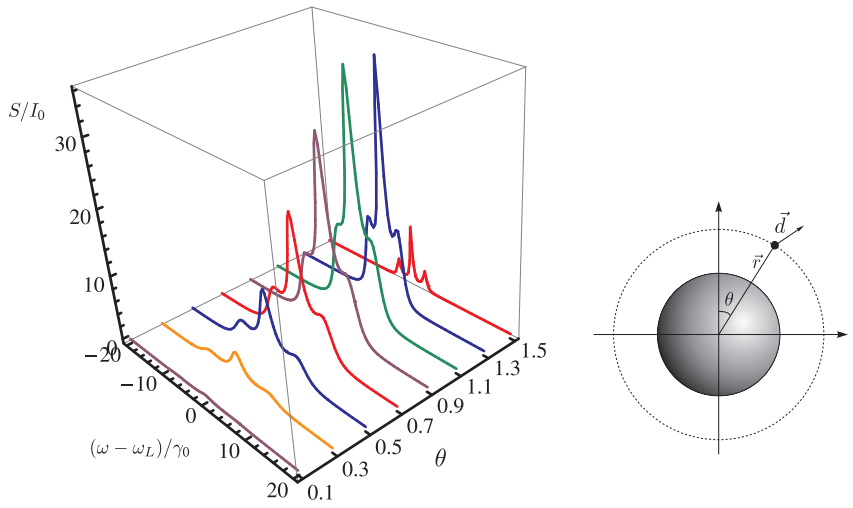

Figure 4: Normalized to I_0 resonance fluorescence spectrum of the two-level atom near the nanosphere of radius $a = 20$ nm versus the angle $\theta = 0.1$–1.5 rad (5.7° to 85.9°, the distance of the atom from the nanosphere surface is equal to 10 nm, $\lambda = 632.8$ nm and $\gamma_0 = 20$ MHz

of the atom's location. The resonance fluorescence spectrum depends on the position of the observer as $S \sim \psi^2$ (see Eq. 14), where ψ is the angle between the atomic dipole direction and z-axis [27].

Figure 5 presents also an analysis of how the resonance fluorescence spectrum depends on the nanosphere radius at the fixed distance between the atom and the nanosphere surface.

The general tendency is that reducing the nanosphere radius leads to the increase of the contrast of the satellite lines in the spectrum.

Calculation of the resonance fluorescence spectrum for N atoms

The case of nanoantenna surrounded by several atoms is of the special interest because it is usual in the experiments. We decide that the atoms don't radiationally interact with each other. The are placed around the nanoantenna so that the potential energy of their mutual interactions is minimal. This is the well known Thomson's problem that have been numerically solved [28, 29].

In this case the full spectrum is the sum of the spectrums from individual atoms. The interaction between atoms is not taken into account.

As it was mentioned above, it is very important to remember about the frequency shift in the case of several atoms. It is clear that the spectrums in this case are more complicated than in the case of a single atom.

Conclusion

In conclusion, we have theoretically investigated modification of the resonance fluorescence spectrum of the two-level atom driven by the monochromatic field in the close proximity of the plasmonic nanostructure (metal sphere). The influence of nanoenvironment was taken into account by using effective (modified by nanoenvironment) values for Rabi frequency and decay rate in a well known expression for the resonance fluorescence spectrum. The result for a single atom were generalized for the case of several atoms.

Finally, a detailed understanding of a single quantum emitter fluorescence, including the resonance fluorescence, modified by the located in close proximity plasmonic nanoparticle is extremely important for the development of nanoscale sensors and biosensing [20, 21], the whole filed of nanoplasmonics [3, 22] and in surface enchanced microscopy and spectroscopy [23, 24, 25, 26]. Moreover, the resonance fluorescence at the nanoscale opens new horizons in studying quantum-optical effects at this scale.

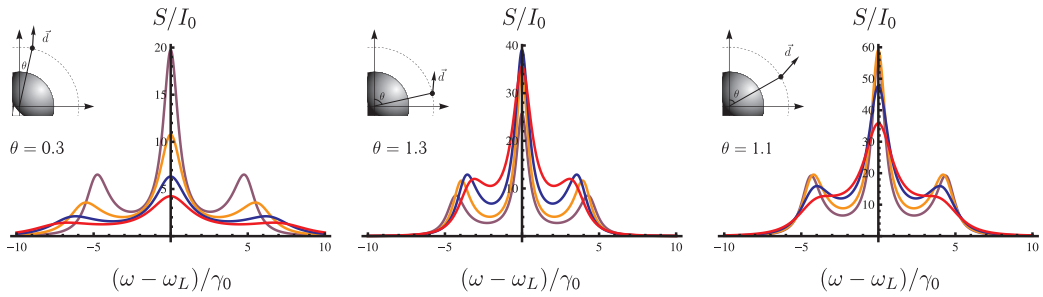

Figure 5: The normalized (to I_0) resonance fluorescence spectrum of the two-level atom near the nanosphere of radius $a = 5$ nm (violet curve), 10 nm (orange curve), 15 nm (blue curve), and 20 nm (red curve) for three locations of the atom with the fixed atom-nanosphere surface distance equal to 10 nm and $\theta = 0.3$ rrad (17°, left figure), 1.3 rad (74.5°, middle figure) and 1.1 rad (63°, right figure); $\lambda = 632.8$ nm and $\gamma_0 = 20$ MHz.

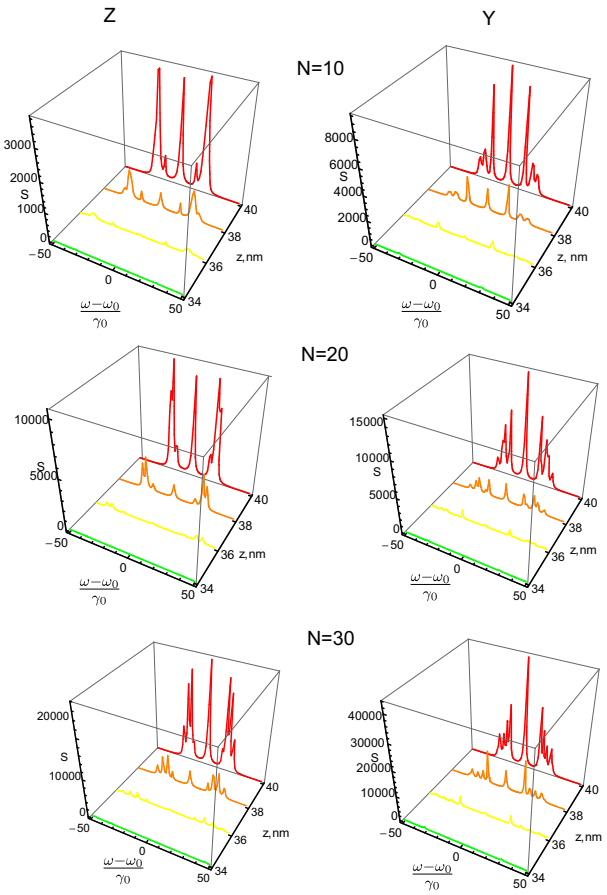

Figure 6: The spectrum for $N = 10, 20, 50$ atoms around the nanosphere for different position of detector. Left figures — detector is on the z-axis, right — on the y-axis

This work was supported by the Federal Program of the Russian Ministry of Education and Science (grant 8393).

References

[1] A. Sommerfeld, Ann. Phys. (Leipzig) **28**, 665736 (1909).

[2] E. M. Purcell, Phys. Rev. **69**, 681 (1946).

[3] V. V. Klimov, *Nanoplasmonics: Fundamentals and applications* (Pan Stanford Publishing, Singapore, 2012).

[4] V. V. Klimov, M. Ducloy, and V. S. Letokhov, Sov. J. Quantum Electron. **31**, 569 (2001).

[5] R. R. Chance, A. Prock, and R. Silbey, Adv. Chem. Phys. **37**, 1 (1978).

[6] R. X. Bian, R. C. Dunn, and X. Sunney Xie, Phys. Rev. Lett. **75**, 4772 (1995).

[7] L. Novotny, Appl. Phys. Lett. **69**, 3806 (1996).

[8] M. Thomas, J.-J. Greffet, R. Carminati, and J. R. Arias-Gonzales, Appl. Phys. Lett. **85**, 3863 (2004).

[9] R. Carminati, J.-J. Greffet, C. Henkel, and J. M. Vigoureux, Optics Commun. **261**, 368 (2006).

[10] J. N. Farahani, D. W. Pohl, H.-J. Eisler, B. Hecht, Phys. Rev. Lett. **95**, 017402 (2005).

[11] B. C. Buchler, T. Kalkbrenner, C. Hettich, and V. Sandoghar, Phys. Rev. Lett. **95**, 063003 (2005).

[12] S. Kühn, G. Mori, M. Aglio, and V. Sandoghdar, Molecular Phys. **106**, 893 (2008).

[13] K. T. Shimizu, W. K. Woo, B. R. Fisher, H. J. Eisler, and M. G. Bawendi, Phys. Rev. Lett. **89**, 117401 (2002).

[14] V. V. Klimov, M. Ducloy, and V. S. Letokhov, J. Mod. Opt. **43**, 2251 (1996).

[15] H. J. Kimble and L. Mandel, Phys. Rev. A **13**, N 6, 2123 (1976).

[16] Such plasmonic nanostructures are technologically made of gold or silver, which are standard materials for optical nanoantennas as they have relatively low losses in optical range of frequencies.

[17] P. A. Apanasevich, Opt. Spectrosc. **16**, 387 (1964).

[18] B. R. Mollow, Phys. Rev. **178**, 1969 (1969).

[19] H. Walther, In: *Advances in Atomic, Molecular and Optical Physics*, Vol. 51, 239 (Elsevier, 2005).

[20] J. N. Anker, W. P. Hall, O. Lyandres, N. C. Shah, J. Zhao, and R. P. van Duyne, Nature Materials **7**, 442 (2008).

[21] T. Sannomiya, J. Vörös, Trends in Biotechnilogy **29**, 343 (2011).

[22] L. Novotny and N. van Hulst, Nat. Photonics **5**, 83 (2011).

[23] S. M. Flores and J. L. Toca-Herrera, Nanoscale **1**, 40 (2009).

[24] F. J. Garcia de Abajo, Rev. of Mod. Phys. **82**, 209 (2010).

[25] A. P. D. Elfick, A. R. Downes, and R. Mouras, Analytical and Bioanalytical Chemistry **396**, 45 (2010).

[26] B. Pettinger, Molecular Phys. **108**, 2039 (2010).

[27] Yu.V. Vladimirova, V.V. Klimov, V.M. Pastukhov, V.N. Zadkov. Phys. Rev. A 85, 053408 (2012).

[28] http://www-wales.ch.cam.ac.uk/ wales/CCD /Thomson/table.html (The Cambridge Cluster Database).

[29] http://math-lab.ru/?i=17